Nanoscale

Accepted Manuscript

This article can be cited before page numbers have been issued, to do this please use: J. Liu, X. Leng, Y. Xiao, C. Hu and L. Fu, *Nanoscale*, 2015, DOI: 10.1039/C5NR03109E.

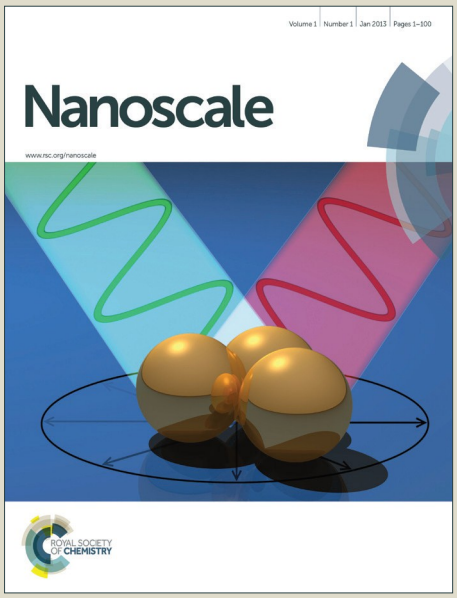

This is an *Accepted Manuscript*, which has been through the Royal Society of Chemistry peer review process and has been accepted for publication.

Accepted Manuscripts are published online shortly after acceptance, before technical editing, formatting and proof reading. Using this free service, authors can make their results available to the community, in citable form, before we publish the edited article. We will replace this *Accepted Manuscript* with the edited and formatted *Advance Article* as soon as it is available.

You can find more information about *Accepted Manuscripts* in the Information for Authors.

Please note that technical editing may introduce minor changes to the text and/or graphics, which may alter content. The journal's standard Terms & Conditions and the Ethical guidelines still apply. In no event shall the Royal Society of Chemistry be held responsible for any errors or omissions in this *Accepted Manuscript* or any consequences arising from the use of any information it contains.

ROYAL SOCIETY OF CHEMISTRY

www.rsc.org/nanoscale

Nanoscale

RSCPublishing

View Article Online
DOI: 10.1039/C5NR03109E

COMMUNICATION

3D nitrogen-doped graphene/β-cyclodextrin: host-guest interaction for electrochemical sensing†

Cite this: DOI: 10.1039/x0xx00000x

Jilun Liu‡, Xuanye Leng‡, Yao Xiao‡, Chengguo Hu, and Lei Fu*

Received 00th March 2015,
Accepted 00th March 2015

DOI: 10.1039/x0xx00000x

www.rsc.org/

Host-guest interaction, especially that between cyclodextrins (CDs, including α-, β- and γ-CD) and various guest molecules, exhibiting a very high supramolecular recognition ability, has received considerable attentions in different fields. The specific interaction between the host and the guest molecules is promising in biosensing and clinical detection. However, there is a lack of an ideal electrode substrate for CDs to exert its performance in electrochemical sensing. Herein, we propose a new 3D nitrogen-doped graphene (3D-NG) based electrochemical sensor take advantage of the superiority sensitivity of host-guest interaction. Our 3D-NG is fabricated by template-directed chemical vapour deposition (CVD) method, which showed large specific surface area, high capacity of biomolecules and fast electron transfer efficiency. Thus, for the first time, we took 3D-NG as an electrode substrate for β-CD to establish a new type biosensors. Using dopamine (DA) and acetaminophen (APAP) as representative guest molecules, our 3D-NG/β-CD biosensors show extremely high sensitivity (5468.6 $\mu A \cdot mM^{-1} \cdot cm^{-2}$ and 2419.2 $\mu A \cdot mM^{-1} \cdot cm^{-2}$, respectively), which are significantly higher than those reported in most previous studies. The stable adsorption of the β-CD on the 3D-NG indicate the potential applications in clinical detection and medical testing.

Introduction

Host-guest interaction was first introduced in 1974.[1] Since then, this concept has attracted considerable attentions of various fields like supramolecular self-assembly[2] and molecular-recognition[3]. And the recognition between host and guest molecules shows a cheerful prospect in electrochemical sensing. Among all potential hosts, CDs seem to be the most important ones because they are environmental-friendly, easy to get at low cost, and most importantly of all, have good inclusion complex forming ability.[4] β-Cyclodextrin (β-CD) is a cyclic oligosaccharide composed by seven α-(1,4) linked glycosyl units and presents a toroidal form with a hydrophobic internal cavity and a hydrophilic exterior.[5] Having a diameter of 6.0~6.5 Å (6.0 Å for the top and 6.5 Å for the bottom),[6] β-CD has the ability to form inclusion complexes with compounds of certain size through host-guest interaction.[7] The principal factors involved in such interaction are believed to be van der Waals forces, hydrophobic interactions, hydrogen bonding and steric effects.[8–11] The formation of the inclusion complexes can exert a profound effect on the physicochemical properties of guest molecules as they are temporarily locked or caged within the host cavity, giving rise to positive modifications of guest molecules,[12] which may be beneficial to the electrochemical features. Though the host-guest interaction concerned with β-CD seems to be potential in electrochemical sensing, it is hard for β-CD itself to accomplish the mission because it would easily detach from the surface of an electrode on which they are modified, let alone its instinct poor conductivity.[13] In recent years, several electrode substrates for β-CD have been reported.[14–18] But we cannot help wondering a more ideal model that is more facile with better performance.

Graphene, a two-dimensional carbon material with fantastic physical and chemical properties,[19-21] has been reported to be used for electrochemical sensing in previous studies.[22-27] However, planar graphene may come across some challenges for its low surface-area-to-volume ratio (sa/vol) and weak interaction with other molecules.[28] So three-dimensional nitrogen-doped graphene (3D-NG) may be an excellent alternative owing to its high sa/vol, satisfactory capacity for biomolecules and high conductivity, which are essential to an electrode substrate to make the utmost of host-guest interaction between β-CD and guest molecules. This 3D structure possesses much higher sa/vol than planar graphene.[29-31] At the same time, the doped nitrogen atoms contribute to the increase of the conductivity and capacity for biomolecules.[28, 31,32]

Herein, we employ 3D-NG as the electrode substrate for β-CD to create a new type biosensor based on host-guest interaction. As is shown in Scheme 1, this structure is similar to the tentacle of an octopus, and the anchored β-CD acted as suckers on its tentacles to catch the guest molecules. This biosensor is confirmed to have a good free-standing structure, high electron transfer efficiency and high capacity for β-CD. To examine its electrochemical performance, we demonstrate the sensing for dopamine (DA, a neurotransmitter, which is important in clinical detection and researches[34]), and acetaminophen (APAP, a kind of widely used anodyne). For the former one, the sensitivity of our sensor was as high as 5468.6 $\mu A \cdot mM^{-1} \cdot cm^{-2}$. And for the latter one the sensitivity also made up to 2419.2 $\mu A \cdot mM^{-1} \cdot cm^{-2}$. These results hint that the high performance for electrochemical sensing is not limited to one specific biomolecule. We believe this kind of biosensors could be used for the detection of various biomolecules which have host-guest interactions with β-CD.

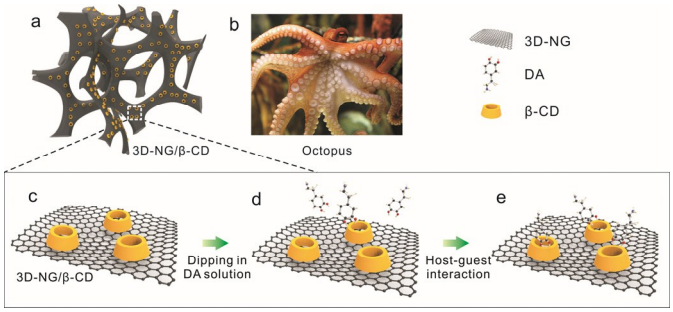

Scheme 1 The loading of β-CD on the surface of 3D-NG and the process of host-guest interaction on the surface of the 3D-NG/β-CD sensor.

Experimental Section

Preparation of the 3D-NG. 3D-NG was synthesized by CVD method using nickel foam (Alantum Advanced Technology Materials, China, 1.65 mm in thickness) of 1.0×1.0 cm^2 as growth substrate. The growth process of 3D-NG was carried out in a quartz tube furnace (HTF 55322C Lindberg/Blue M) under atmospheric pressure. This process consisted of four steps: (1) nickel foams were heated to 1000 °C from around 25 °C within 30 min under the gas flow of Ar (500 sccm) and H_2 (200 sccm), (2) annealed at 1000 °C for 5 min to make the nickel surface clean and smooth, (3) exposed to the gas flow of methane (CH_4, 10 sccm), ammonia (NH_3, 14 sccm) and Ar (500 sccm) for another 5 min under 1000 °C, and (4) cooled down to room temperature at a rate of 30 °C min^{-1} under only Ar (500 sccm). After the growth procedure, the foams were etched in HNO_3 (1.3 M) for 12 h. At last, the 3D-NG was rinsed by ultrapure water for 80 min to remove the residual of ions. The preparation of 3D-G was in the same way except that NH_3 was not introduced into the reaction tube during the third step. The procedure was slightly modified from our previous work.[35]

Fabrication of the 3D-NG/β-CD biosensor. β-CD powder (Sinopharm Chemical Reagent Co., Ltd, China) was added into ultrapure water to obtain saturated CD solution. The free-standing 3D-NG or 3D-G was then immersed in this solution and ultrasonicated for 30 min. An extra 12 h of immersion in the saturated solution was taken to maximize the loading effect. The CD solution remaining on the 3D-NG or 3D-G surface was removed by ultrapure water. Thereafter, the 3D-G, 3D-NG, 3D-G/β-CD or 3D-NG/β-CD were fixed onto a piece of PET (polyethylene terephthalate) substrate respectively. Then a copper wire was bonded to the 3D-NG or 3D-G by silver paint and insulated with epoxy resin. More detailed information can be found in Fig. S1. (ESI†).

Characterization. Raman spectroscopy was carried out with a laser micro-Raman spectrometer (Renishaw inVia, Renishaw, 532 nm excitation wavelength). X-ray photoelectron spectroscopy (XPS) was performed on Thermo Scientific, ESCALAB 250Xi. X-Ray diffraction (XRD) measurements were taken on a LabX XRD-6000 using Cu-Kα radiation over the range of 2θ = 10~80°. Thermo gravimetric analysis (TGA) was performed on TGA-500. Scanning electron microscopy (SEM) was taken on a ZEISS Sigma. Electrochemical impedance spectroscopy (EIS) was carried out with a Model 283 potentiosata/galvanostat and Model 5210 lock-in amplifier.

View Article Online
DOI: 10.1039/C5NR03109F

Electrochemical measurements. Cyclic voltammograms (CV) were obtained with a CHI 660a electrochemical working stat... (Chenhua, China). A three-electrode system was employed. 3D NG/β-CD electrode was the working electrode. At the sam... time, a platinum foil and a saturated calomel electrode (SCE) served as the counter electrode and the reference electrode, respectively. Dopamine hydrochloride (98%) was purchas... from Aladdin Industrial Corporation, China and acetaminophen (CP grade) were purchased from form Sinopharm Chemic... Reagent Co., Ltd, China.

Results and discussion

Characterization of 3D-NG and 3D-G. Raman spectrum is a... effective tool to identify the quality and doping effect o... graphene.[36,37] Fig. 1 shows different Raman spectra of 3D-G 3D-NG, β-CD and 3D-NG/β-CD. For pristine 3D-G, there is a strong G band at 1581 cm^{-1} and a relatively weaker 2D band ... 2702 cm^{-1}, indicating that 3D-G is multilayered. For 3D-NG, a D band locates at 1356 cm^{-1}, which often represents the def... on the surface including boding disorders and vacancies in the graphene lattice that are induced by nitrogen doping.[37] After ... loading of β-CD molecules, the typical bands of β-CD overlay with those of 3D-NG.

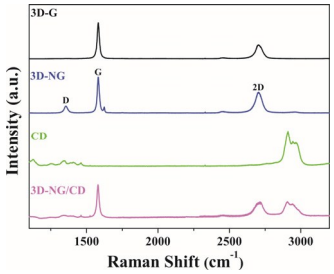

Fig. 1 Typical Raman spectra of 3D-G, 3D-NG, β-CD and 3D-NG/β-CD.

XPS was used to further investigate the doping effect. A... shown in Fig. S2 (ESI†), the 3D-NG has a prominent N 1s peak whereas no detectable N peaks can be found in the 3D-G sample. Its N/C atomic ratios estimated by XPS is 4.40 %. Th... N1s peak can be split into three individual components centre... at 398.0 eV, 398.1 eV and 398.4 eV (Fig. 2a), which are attributed to pyridinic N (N1), pyrrolic N (N2), and graphitic N (N3), respectively.[39,40] As is shown in Fig. 2b, the mo... prominent peak of C1s is located at 284.6 eV (C1), corresponding to the graphite-like sp^2 C; while small peaks ... 285.1 eV (C2) and 286.0 eV (C3) are clearly visualized i... addition to the main peak, reflecting two different bonds corresponding to the N-sp^2 C and N-sp^3 C, respectivel... originating from the substitutional doping of N atoms.[38,41] The C1s peak at 290.7 eV (C4) is attributed to CO type bond. Th... doping of nitrogen will greatly enhance the loading of β-CD molecules on the graphene surface because that graphitic N atoms interact with β-CD molecules through hydrogen bond... and other weak interactions.

The XRD patterns of 3D-G and 3D-NG structures (Fig. S3, ESI†) both exhibit a strong [002] graphitic peak at 26.5°, indicating a high crystalline degree both before and after nitrogen-doping.

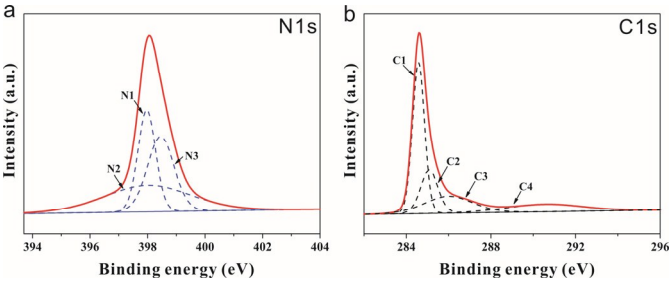

Fig. 2 XPS spectra of 3D-NG: (a) N1s spectra and (b) C1s spectra.

Characterization of 3D-NG/β-CD biosensor. The morphology of the samples was characterized by SEM. As shown in Fig. 3a, 3D-NG exhibits a well-defined macroporous structure and remains free-standing after etching and ultrasonication, confirming its potential as a substrate for fabricating biosensor. The high-magnification SEM image shows a smooth surface of the 3D-NG with some wrinkles but no cracks, indicating a continuous connection between the graphene sheets (Fig. 3b). After immersion and ultrasonication in a β-CD solution, the structure of the 3D skeleton can also be well maintained (Fig. 3c). From Fig. 3d, we can see that the surface is mostly covered with a film of β-CD, indicating a large number of β-CD are adsorbed on the surface. In addition, due to the large surface area of the 3D porous structure, the load of β-CD could be extremely high.

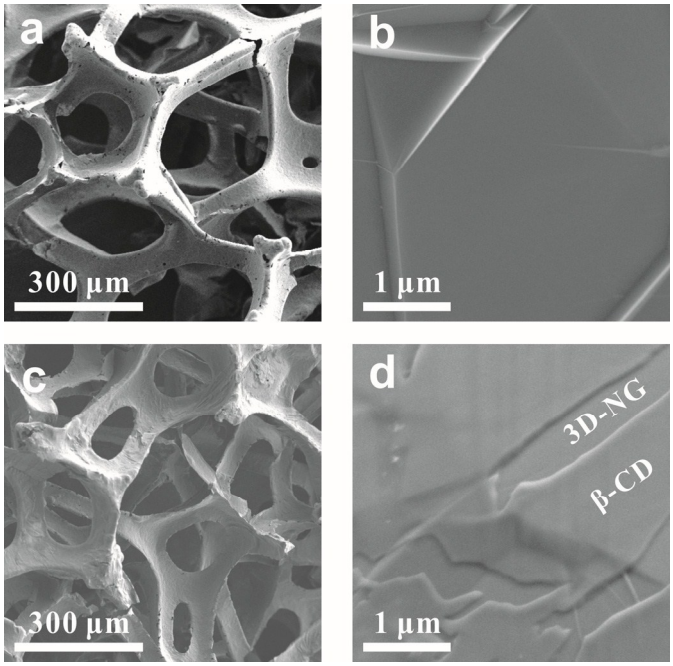

Fig. 3 SEM images: low-magnification images of (a) 3D-NG and (c) 3D-NG/β-CD; high-resolution images exhibiting the surface of (b) 3D-NG and (d) 3D-NG/β-CD.

TGA was used to determine the amount of β-CD molecules carried by 3D-NG. As is shown in Fig. 4a, there is a major weight loss of pure β-CD at about 300 °C under a nitrogen flow, which should be attributed to the decomposition of β-CD. Accordingly, the weight loss of 3D-G/β-CD and 3D-NG/β-CD at this temperature indicates that the amount of β-CD molecules carried by 3D-G was about 16 wt% while that of 3D-NG was about 30 wt%. The weight of pure 3D-G and 3D-NG almost remained unchanged throughout the temperature-rise period. Apparently, 3D-G could carry plenty of β-CD molecules thanks to its large specific surface area brought by the three-dimensional structure. A hydrogen-bond (N···H−O) attraction can occur between 3D-NG and the oxhydryl groups of β-CD. As a result, 3D-NG has a much higer capacity of β-CD as mentiond above.

View Article Online
DOI: 10.1039/C5NR03100F

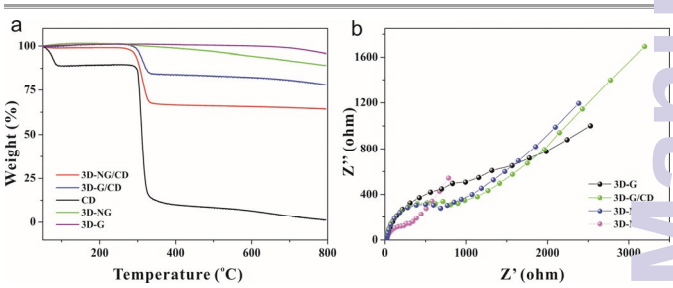

Fig. 4 (a) TGA curves of 3D-NG/β-CD, 3D-G/β-CD, β-CD, 3D-NG and 3D-G. (b) EIS plots of 3D-G, 3D-G/β-CD, 3D-NG and 3D-NG/β-CD. EIS experiments were conducted in 0.1M KCl solution which contained 2.5 mM $K_3Fe(CN)_6$ and 2.5 mM $K_4Fe(CN)_6$.

The electrochemistry of 3D-NG/β-CD biosensor. EIS was carried out to determine the charge-transfer resistance as indicated directly by the diameter of the preceding semicircle in Nyquist plot. As is shown in Fig. 4b, the charge transfer resistance of 3D-NG is smaller than that of 3D-G and 3D-NG/β-CD brings a much smaller one. Graphitic N could increase the conductivity, facilitating the transfer of electrons. And the loading of β-CD molecules may further enhance the transfer efficiency.

To reveal the dynamic mechanism of reactions on the electrode surface, the effect of scan rate on the peak current was tested by CV measurements. A linear relationship between peak current and square root of different scan rate illustrates that the reaction at the 3D-NG/β-CD electrode is a diffusion controlled process. And the detail is given in the Fig. S4 (ESI†).

CV method was further taken to determine the performance of this biosensor. As is shown in Fig. 5a, in DA solution, no oxidation peak current could be found on bare 3D-G while there was one on 3D-G/β-CD, indicating that β-CD conduced to the electrochemical response of DA. Compared to bare 3D-G, 3D-NG performed a relatively higher current. Most importantly, of all, 3D-NG/β-CD had a remarkable increase of peak current which could be understood as follows: (1) the electrochemical response should be contributed to the host-guest interaction because it hardly showed up at the absence of β-CD; (2) nitrogen doping significantly increased the electron transfer efficiency and the capacity for loading β-CD molecules. The comparison was also taken in APAP solution and the result further verified our inference (Fig. 5b). To determine the sensitivity of our biosensors for these two biomolecules, the voltammograms was also obtained, as is exhibited in Fig. 5c. The electrochemical responses of the 3D-NG/β-CD sensor to DA with various concentrations from 10 to 250 μM was

obtained. As is shown in the calibration curve (Fig. 5d), the plot of i_{pa} *versus* DA concentration has good linearity when the concentration is from 10 to 140 μM. The linear regression equation is calculated to be i_{pa} (μA) = 4.8723 + 0.8695 C_{DA} (μM), with a correlation coefficient of 0.9965. The sensitivity of the 3D-NG/β-CD sensor is calculated to be 5468.6 $\mu A \cdot mM^{-1} \cdot cm^{-2}$. The same sensing was taken to APAP to confirm that the high sensitivity is not occasional. Fig. 5e exhibits the voltammetric responses of the 3D-NG/β-CD electrode to the APAP with various concentrations from 10 to 350 μM. As is shown in the calibration curve (Fig. 5f), the plot of i_{pa} versus APAP concentration also has good linearity when the concentration is from 10 to 250 μM and the linear regression equation is i_{pc} (μA) = 0.8507 + 0.3041 C_{APAP} (μM) with a correlation coefficient of 0.9935. The sensitivity of the 3D-NG/β-CD sensor is calculated to be 2419.2 $\mu A \cdot mM^{-1} \cdot cm^{-2}$. Comparing to the sensitivity data reported in previous studies (Tab. S1, ESI†), our results are at least three times higher, indicating the excellent performance of our biosensors.

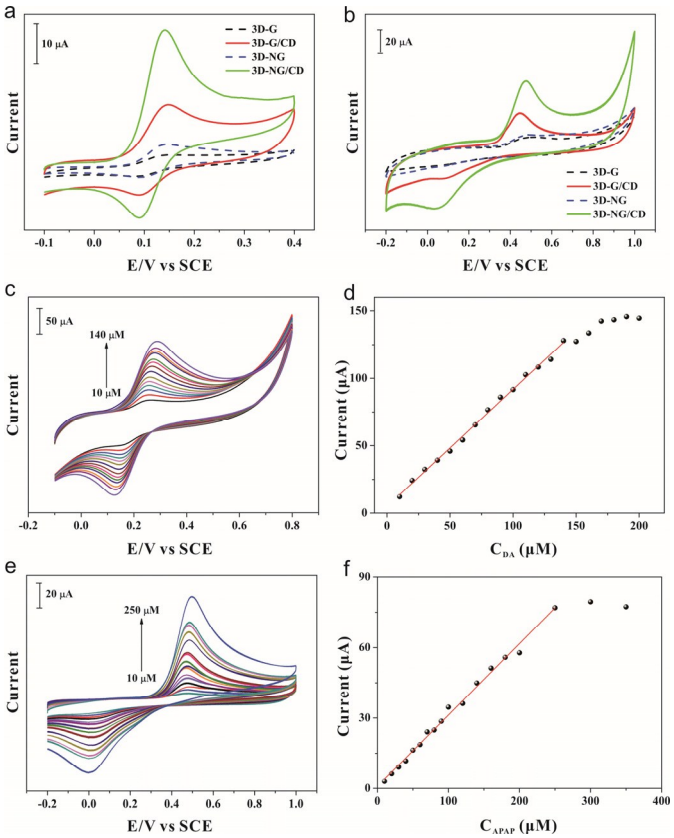

Fig. 5 CV of different electrodes in (a) 100 μM DA and (b) 100 μM APAP. (c) CV of 3D-NG/β-CD 0.1 M PBS (pH = 6.00) containing various DA concentrations from 10 to 250 μM. (e) CV 0.2 M PBS (pH = 7.20) containing various APAP concentrations from 5 to 350 μM. The scan rate was 100 $mV \cdot s^{-1}$. And calibration curve corresponding to the cathodic peak current responses of the 3D-NG/β-CD sensor to various concentrations of (d) DA and (f) APAP.

It has been reported that the diameter of α-CD is 4.7 Å and 5.3 Å for the top and bottom, respectively.[6] This cavity is suitable for benzene molecule with which to form a inclusion complex.[5] But for benzene derivatives that have functional groups enlarging the size, the cavity of α-CD is not enough anymore. Hence, β-CD with a diameter of 6.0~6.5 Å may be a great host for detecting benzene derivatives. Based on the results above, DA and APAP can both interact with β-CD and form inclusion complexes. For DA, the interactions may result from hydrogen bonds between hydroxyl groups of DA and ether oxygen groups of β-CD. On the other hand, a weak acidic environment may turn the amino into ionic ammonium and make it possible for ion-polar interaction between DA and β-CD. When it comes to APAP, there also lays the possibility for hydrogen bonds to form because of the acetyl amino group. On bare 3D-G or 3D-NG surface, the electrochemical process of DA and APAP is not efficient because the direct interaction between the small molecule and the substrate is weak and the electron transfer is limited. But after the interaction between a guest molecule and β-CD, the guest molecules are locked into the cavity and a supramolecular system is established. The β-CD molecules loaded on the electrode substrate make it easier for electrons to transfer between the guests and the electrode. As a result, the response current increases.

View Article Online
DOI: 10.1039/C5NR03109S

Furthermore, to test the stability of the 3D-NG/β-CD sensor, a repeating CV measurement was carried out. As is shown in Fig. S5 (ESI†), the relative standard deviation (RSD) is 2.35%. The response current could remain steady because the interaction between 3D-NG and β-CD is very strong and the biosensor system could work stable. To testify the selectivity of our sensor in the potential applications, ascorbic acid (AA) was introduced in the detecting procedure of DA and there was no obvious signal of AA (100 μM) detected, as is shown in Fig. S6 (ESI†). Last but not least, this 3D-NG/CD sensor is not limited to detect DA and APAP. Indeed, other guest molecules with appropriate size could also be detected with high sensitivity, as shown in Fig. S7 (ESI†).

Conclusions

In summary, 3D-NG was fabricated by CVD method and served as the electrode substrate for β-CD. 3D-NG had large specific surface area, high conductivity and satisfactory capacity for CD while host-guest interaction between β-CD and various guest molecules. Our 3D-NG sensor showed a great performance in electrochemical sensing. For DA and APAP, the sensitivities of our biosensor were 5468.6 $\mu A \cdot mM^{-1} \cdot cm^{-2}$ and 2419.2 $\mu A \cdot mM^{-1} \cdot cm^{-2}$, respectively. This result was significantly higher than most previous studies. Also, a series of repeating experiments, of which RSD = 2.35 %, indicated this new biosensor to be stable, on which β-CD molecules would not be detached easily. So we envision that our biosensor has the potential to be applied in clinical detection and medical testing.

Acknowledgements

This study was supported by the Natural Science Foundation of China (Grants 51322209, 21473124), the Sino-German Center for Research Promotion (Grants GZ 871), the Ministry of Education (Grants 20120141110030) and Fundamental Research Funds for the Central Universities (Grants 2042014kf0244).

Reference

College of Chemistry and Molecular Science, Wuhan University, Wuhan, 430072, China.
*Email: leifu@whu.edu.cn.
†Electronic Supplementary Information (ESI) available: The procedure of preparing the sensor, wide survey XPS, XRD patterns and the effect of

scan rate, more CV data on stability, selectivity and a comparison with previous studies. See DOI: 10.1039/b000000x/
‡ These authors contributed equally to this work.

1. D. J. Cram and J. M. Cram, *Science*, 1974, **183**, 803−809.
2. R. M. Yebeutchou, F. Tancini, N. Demitri, S. Geremia, R. Mendichi and E. Dalcanale, *Angew. Chem., Int. Ed.*, 2008, **47**, 4504−4508.
3. M. D. Pluth and K. N. Raymond, *Chem. Soc. Rev.*, 2007, **36**, 161−171.
4. J. Szejtli, *Chem. Rev.*, 1998, **98**, 1743−1753.
5. M. V. Rekharsky and Y. Inoue, *Chem. Rev*., 1998, **98**, 1875−1917.
6. S. Li and W. C. Purdy, *Chem. Rev*., 1992, **92**, 1457−1490.
7. S. D. Eastburn and B. Y. Tao, *Bio. Adv.*, 1994, **12**, 325−339.
8. D. Hallén, A. Schön, I. Shehatta and I. Wadsö, *J. Chem. Soc., Faraday Trans*., 1992, **88**, 2859−2863.
9. Y. Matsui and K. Mochida, *Bull. Chem. Soc. Jpn.*, 1979, **52**, 2808−2814.
10. W. Saenger, *Angew. Chem., Int. Ed. Engl*, 1980, **19**, 344−362.
11. I. Tabushi, Y. Kiyosuke, T. Sugimoto and K. Yamamura, *J. Am. Chem. Soc*., 1978, **100**, 916−919.
12. G. Schmid, *Trends Biotechnol*., 1989, **7**, 244−248.
13. Y. J. Guo, S. J. Guo, J. T. Ren, Y. M. Zhai, S. J. Dong and E. K. Wang, *ACS Nano*, 2010, **4**, 4001−4010.
14. G. Alarcón-Angeles, B. Pérez-López, M. Palomar-Pardave, M. T. Ramírez-Silva, S. Alegret and A. Merkoçi, *Carbon*, 2008, **46**, 898−906.
15. C. Camacho, J. C. Matías, B. Chico, R. Cao, L. Gómez, B. K. Simpson and R. Villalonga, *Electroanalysis*, 2007, **19**, 2538−2542.
16. M. Holzinger, L. Bouffier, R. Villaonga and S. Cosnier, *Biosens. Bioelectron.*, 2009, **24**, 1128−1134.
17. D. Du, M. H. Wang, J. Cai and A. D. Zhang, *Sens. Actuators B*, 2010, **146**, 337−341.
18. X. M. Xu, Z. Liu, X. Zhang, S, Duan, S. Xu and C. L. Zhou, *Electrochim. Acta*, 2011, **58**, 142−149.
19. Y. Liu, X. C. Dong and P. Chen, *Chem. Soc. Rev.*, 2012, **41**, 2283−2307.
20. X. Huang, Z. Y. Yin, S. X. Wu, X. Y. Qi, Q. Y. He, Q. C. Zhang, Q. Y. Yan, F. Boey and H. Zhang, *Small*, 2011, **7**, 1876−1902.
21. X. Huang, X. Y. Qi, F. Boey and H. Zhang, *Chem. Soc. Rev.*, 2012, **41**, 666−686.
22. Z. P. Chen, W. C. Ren, L. Gao, B. L. Liu, S. F. Pei and H. M. Cheng, *Nat. Mater.*, 2011, **10**, 424−428.
23. Y. Y. Shao, J. Wang, H. Wu, J. Liu, I. A. Aksay and Y. H. Lin, *Electroanalysis*, 2010, **22**, 1027−1036.
24. R. S. Dey and R. Raj. *Biosens. Bioelectron.*, 2014, **62**, 357−364.
25. S. X. Wu, Q. Y. He, C. L. Tan, Y. D. Wang and H. Zhang, *Small*, 2013, **9**, 1160−1172.
26. Z. J. Wang, X. Z. Zhou, J. Zhang, F. Boey and H. Zhang, *J. Phys. Chem. C*, 2009, **113**, 14071−14075.
27. Z. J. Wang, J. Zhang, P. Chen, X. Z. Zhou, Y. L. Yang, S. X. Wu, L. Niu, Y. Han, L. H. Wang, P. Chen, F. Boey, Q. C. Zhang, B. Liedberg and H. Zhang, *Biosens. Bioelectron.*, 2011, **26**, 3881−3886.
28. A. R. Fei, Q. Liu, J. Huan, J. Qian, X. Y. Dong, B. J. Qiu, H. P. Mao and K. Wang, *Biosens. Bioelectron.*, 2015, **70**, 122−129.
29. X. H. Cao, Z. Y. Zeng, W. H. Shi, P. Yep, Q. Y. Yan and H. Zhang, *Small*, 2013, **9**, 1703−1707.
30. X. H. Cao, Y. M. Shi, W. H. Shi, X. H. Rui, Q. Y. Yan, J. Kong and H. Zhang, *Small*, 2013, **9**, 3433−3438.
31. Z. J. Wang, X. H. Cao, J. F. Ping, Y. X. Wang, T. T. Lin, X. Huang, Q. L. Ma, F. K. Wang, C. B. He and H. Zhang, *Nanoscale*, 2015, **7**, 9394−9398.
32. L. Sun, L. Wang, C. Tian, T. Tan, Y Xie, K. Shi, M. Li and H. Fu, *RSC Adv*., 2012, **2**, 4498−4506.
33. Y. H. Xue, D. S. Yu, L. M. Dai, R. G. Wang, D. Q. Li, A. Roy, F. Lu, H. Chen, Y. Liu and J. Qu, *Phys. Chem. Chem. Phys.*, 2013, **15**, 12220−12226.
34. S. R. Ali, Y. F. Ma, R. S. R. Parajuli, Y. Balogun, W. Y. C. Lai and H. X. He, *Anal. Chem.*, 2007, **79**, 2583−2587.
35. J. X. Guo, T. Zhang, C. G. Hu and L. Fu, *Nanoscale*, 2015, **7**, 1290−1295.
36. M. S. Dresselhaus, A. Jorio, A. G. Souza Filho and R. Saito, Philos, *Trans. R. Soc. A*, 2010, **368**, 5355−5377.
37. A. C. Ferrari, J. C. Meyer, V. Scardaci, C. Casiraghi, M. Lazzeri, F. Mauri, S. Piscanec, D. Jiang, K. S. Novoselov, S. Roth and A. K. Geim, *Phys. Rev. Lett.*, 2006, **97**, 187401−187404.
38. C. H. Zhang, L. Fu, N. Liu, M. H. Liu, Y. Y. Wang and Z. F. Liu, *Adv. Mater.*, 2011, **23**, 1020−1024.
39. R. J. J. Jansen and H. van Bekkum, *Carbon*, 1995, **33**, 1021−1027.
40. Y. Nakayama, F. Soeda and A. Ishitani, *Carbon*, 1990, **28**, 21−26.
41. D. C. Wei, Y. Q. Liu, Y. Wang, H. L. Zhang, L. P. Huang and G. Yu, *Nano Lett.*, 2009, **9**, 1752−1758.